Gait Abnormality Detection in People with Cerebral Palsy using an Uncertainty-based State-space Model

Saikat Chakraborty, Noble Thomas, and Anup Nandy

Machine Intelligence and Bio-motion Research Lab,
Department of Computer Science and Engineering,
National Institute of Technology, Rourkela, Odisha, India

Abstract. Assessment and quantification of feature uncertainty in modeling gait pattern is crucial in clinical decision making. Automatic diagnostic systems for Cerebral Palsy gait often ignored the uncertainty factor while recognizing the gait pattern. In addition, they also suffer from limited clinical interpretability. This study establishes a low-cost data acquisition set up and proposes a state-space model where the temporal evolution of gait pattern was recognized by analyzing the feature uncertainty using Dempster-Shafer theory of evidence. An attempt was also made to quantify the degree of abnormality by proposing gait deviation indexes. Results indicate that our proposed model outperformed state-of-the-art with an overall 87.5% of detection accuracy (sensitivity 80.00%, and specificity 100%). In a gait cycle of a Cerebral Palsy patient, first double limb support and left single limb support were observed to be affected mainly. Incorporation of feature uncertainty in quantifying the degree of abnormality is demonstrated to be promising. Larger value of feature uncertainty was observed for the patients having higher degree of abnormality. Sub-phase wise assessment of gait pattern improves the interpretability of the results which is crucial in clinical decision making.

Keywords: Dempster-Shafer theory, Uncertainty, Kinect, Cerebral Palsy

1 Introduction

Cerebral Palsy (CP) is a neurological disorder attributed to non-progressive damage of fetal or infant brain, causing limited movement and postural instability [1]. Around the world, more than 4 per 1000 children suffer from CP [2]. In developing countries the prevalence of CP is alarming. For example, in India, more than $15 - 20\%$ of physically disabled children are suffering from CP [3]. Proper therapeutic intervention can improve the quality of gait in children with CP [4]. Hence, the diagnosis of gait pattern is crucial in investigating the efficacy of an intervention [5].

Approaches for machine learning (ML)-based automated gait diagnosis can be broadly divided into two groups: feature-based classification technique and cycle segmentation-based state-space modeling technique. Feature-based techniques

ICCS Camera Ready Version 2020
To cite this paper please use the final published version:
DOI: 10.1007/978-3-030-50423-6_40

require extraction of a suitable set of features which is highly depended on expert knowledge or network architecture type (in deep learning). Despite providing satisfactory performances this strategy of diagnosis suffers from low clinical interpretability of the outcome [6]. In clinical diagnosis, the interpretability of the results carries more importance than just reporting classification accuracy [7]. On the other hand, state-space models recognize the gait pattern by temporal segmentation of a gait cycle. It provides sub-phase wise comprehensive gait analysis with relevant clinical interpretation [8]. Characterization of gait signal in each sub-phase unfolds the spatio-temporal evolution of the system dynamics over a period of time.

In coordinative movement, the uncertainty in prediction of the initial state of system dynamics impacts the measurement of gait variables (i.e. features) [9]. Decision relating to the assignment of a class level (i.e. normal or abnormal) using such a feature set associates a level of uncertainty [10]. Quantification of this uncertainty is crucial in clinical decision making [10]. In literature, different studies have demonstrated automated gait diagnosis system for people with CP [5, 11–13]. However, the analysis of feature uncertainty in decision making was often ignored. Dempster-Shafer theory of evidence (DST) [14, 15] has been successfully used to map the uncertainty in the classification process [16–18] in different problem domains. It assign a mass probability to particular class considering the uncertainty factor associated with the evidence. Hence, the use of DST in classifying CP gait seems to be promising and clinically viable. Again, an investigation of the impact of each of gait sub-phases on the overall abnormal gait pattern of CP patients seems warranted. Another fact is that, the existing automated CP gait diagnostic systems associates high-cost sensors which make the overall system expensive. Most of the clinics, specially in developing countries, are not able to afford those costly systems. Thus, a low-cost automated diagnosis system is also needed for people with CP.

This study aimed to construct a novel state-space based automated gait diagnosis system for children and adolescent with CP (CAwCP) by quantifying uncertainty of the selected feature set. First, a low-cost sensor-based architecture was proposed from which velocity of ankle joints were extracted. Second, a state-space model was build where state duration and transition was modeled using DST. Variability of state duration was used to recognize the gait pattern. The use of DST allows the presence of uncertainty in gait velocity. Quantification and incorporation of this uncertainty facilitated subject specific gait modeling. Third, an index for quantification of the degree of abnormality was also proposed. Finally, state-of-the-art feature-based gait classification approaches were compared with the proposed system. The contributions of this work are as follows:

- Establishing a low-cost multi-sensor-based architecture for data acquisition.
- Developing a state-space model for automated gait diagnosis for CAwCP that incorporate uncertainty of features to estimate the temporal evolution of signal.
- Proposing degree of abnormality indexes based on dynamic stability and feature uncertainty.

ICCS Camera Ready Version 2020
To cite this paper please use the final published version:
DOI: 10.1007/978-3-030-50423-6_40

The rest of the paper is organized as follows: section 2 describes elaborately the state-of-the-art methods to detect CP gait abnormality. Construction of a low-cost architecture for data acquisition, description of the proposed state-space model and degree of abnormality indexes are demonstrated in section 3. Section 4 presents the results with an elaborate discussion. The paper concludes in section 5 by providing a future research direction.

2 Related Work

Several attempts have been made to construct automated gait diagnostic system for CP patients.
Kamruzzaman et al. [5] proposed an automated gait diagnosis system for children with CP (CwCP) using support vector machine (SVM). Normalized stride length and cadence were used as an input features for the classifier. They reported SVM as comparatively better classifier with an overall abnormality detection accuracy of 96.80%. Wolf et al. [13] accumulated gait data from different sensors and constructed a large feature pool by gait sub-phases analysis. Features were ranked using mutual information and then used for fuzzy rule-based classification. A gait deviation index was also introduced in their study. Zhang et al. [11] investigated the significance of Bayesian classifier to diagnosis CP patients. They computed normalized stride length and cadence and reported Bayesian classifier as better than other popular classifiers. Gestel et al.[19] used Bayesian networks (BN) in combination with expert knowledge to form an semi-automated diagnostic system. They reported a promising detection accuracy (88.4%) using sagittal plane gait dynamics. Laet et al. [12] obtained joint motion pattern from Delphi-consensus study [20] and used it to detect CP gait using Logistic Regression and nave Bayes classifiers. They recommended the inclusion of expert knowledge in feature selection and discretization of continuous features to detect gait abnormality. Zhang et al. [21] extracted a set of crucial kinematic parameters from sagittal plane gait pattern of CwCP and given it as input to seven popular supervised learning algorithms. They reported artificial neural network (ANN) as the best model followed by SVM, decision tree (DT), and random forest (RF). Krzak et al. [22] collected kinematic gait parameters of people with CP using Milwaukee Foot Model (MFM). They applied k-means clustering and obtained five distinct groups having similar gait pattern. Dobson et al. [23] and recently Papageorgiou et al. [24] have thoroughly analyzed the automated classification systems available for CP patients and reported cluster-based algorithms as the most used technique for gait detection in CP patients. But, cluster-based models may construct clinically irrelevant artificial group and suffer from limited clinical interpretations [21]. Though the above mentioned models have obtained satisfactory results, they have ignored the uncertainty factor associated with the feature set which is crucial in deciding the class label. Again, those systems are highly expensive also.

ICCS Camera Ready Version 2020
To cite this paper please use the final published version:
DOI: 10.1007/978-3-030-50423-6_40

Table 1. Demographic information of the subjects *

Participants (N=30)	CP type	GMFCS levels	Age (years)	Height (cm)	Gender
CAwCP (15)	Diplegic:5	I, II	11.71 ± 4.46	124.00 ± 16.92	M:3, F:2
	Hemiplegic (RS):5	II	10.84 ± 3.6	114.66 ± 15.28	M:2, F:3
	Hemiplegic (LS):3	I, II	12.00 ± 6.38	132.25 ± 20.17	M:2, F:1
	Athetoid:2	I, II	15.66 ± 2.52	149.67 ± 5.51	M:1, F:1
			12.55 ± 2.13	130.15 ± 14.87	M:8, F:7
TDCA (15)			12.45 ± 3.51	132.06 ± 14.09	M:9, F:6
P-value			0.78	0.27	0.71

*GMFCS: Gross Motor Function Classification System, RS: Right side, LS: Left side, M: male, F: female

3 Methods

3.1 Participants

Fifteen CAwCP patients, without having any other disease or surgical history that can affect the gait pattern, and who can walk without any aid, were recruited from the Indian Institute of Cerebral Palsy (IICP), Kolkata. Along with that, fifteen typically developed children and adolescent (TDCA) without having any type of musculoskeletal or neurological disease that can affect gait pattern, also were recruited. This work was approved by the ethics board of local institution. The objectives and protocols of our experiment were explained to the participants and an informed consent form was signed from each of them. Table 1 shows the demographic information of the subjects which demonstrates that there was no significant difference ($p > 0.05$) between the two groups in terms of anthropometric parameters.

3.2 Experimental setup and data acquisition

We have used low-cost Kinect (v2) sensor for data acquisition which make our proposed system cost-effective. Inspired by the work of Geerse et al. [25] we have constructed a three Kinect-based client-server architecture (see figure 1) which covers $10m$ walking distance. The Kinects were placed on tripods (Slik F153) sequentially at 35° angle with the walking direction. The arrows emerging from Kinects cover the horizontal field of view (FoV) of Kinect i.e. 70° [26]. The distance of the Kinects from the left border of the track was $2m$. Height and tilt angle of the Kinects were $0.8m$ and 0° respectively, while the distance between the Kinects was $3.5m$. The width of the track was $0.84m$. This setup allowed $\approx 0.5m$ of overlapped tracking volumes (between two successive sensors) which was empirically estimated to be sufficient (for both the groups) for the next sensor to recognize a person's body and start tracking. A computer was set as the server which controlled each of the Kinect connected to separate computers. System clocks of the computers were synchronized using Greywares DomainTime II

ICCS Camera Ready Version 2020
To cite this paper please use the final published version:
DOI: 10.1007/978-3-030-50423-6_40

(Greyware Automation Products, Inc.), which follows PTP protocol. A training session was provided to the participants before the experiment. Subjects were asked to start walk at self selected speed from $4m$ distance from the 1^{st} Kinect and after walking $1m$ distance (marked by line) data were started to capture. Subjects were asked to walk upto the 'End' line. The total distance of the path was $12m$ out of which $10m$ distance was considered for data collection. The extra distances (at start and ending points) were given to reduce the effect of acceleration and deceleration on gait variables. Five trials for each participants were taken with 2 min of resting gap. The client-server architecture followed the same protocol like [25, 26] to record, combine, remove noise, and process body point data series from multiple Kinects.

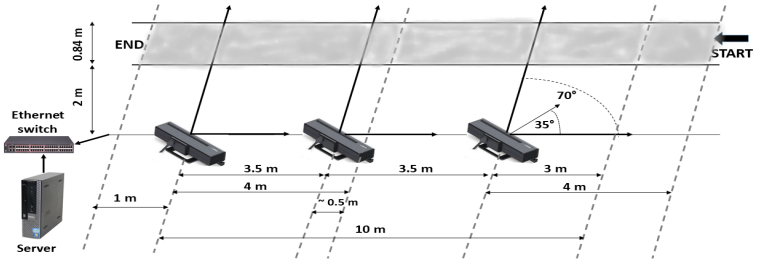

Fig. 1. Data acquisition in multi-Kinect environment

3.3 Dempster-Shafer Classifier

Our proposed state-space model was constructed by estimating uncertainty of feature using DST. This section describes the theoretical ground of DST for using it as a classifier, often termed as *Cardiff Classifier* [17].
The Cardiff classifier is constructed on the basis of some elementary and mutually exclusive hypotheses which constitute the frame of discernment (FOD) [16]. If there are two elementary hypotheses, for e.g. h: belongs to class i, and $\neg h$: not belongs to class i, then FOD is called binary frame of discernment (BFOD), denoted as Θ. There are 4 number of possible hypotheses derived from the elementary hypotheses: $\{\{\varnothing\}, \{h\}, \{\neg h\}, \{h, \neg h\}\}$. On the basis of existing evidence, each hypothesis is assigned a probability mass value $m(.)$ which is called degree of belief (DOB) [16]. It refers the strength of support for a classification. Each of the hypotheses $\{\theta_i\}$, $(i = 1, ..., 2^{|\Theta|})$ having $m(\theta_i) > 0$ constitute body of evidence (BOE) [16, 10]. The basic property of $m(.)$ is given by [27]:

$$0 \leq m(.) \leq 1, m(\varnothing) = 0, \sum_{i=1}^{2^{|\Theta|}} m(\theta_i) = 1 \tag{1}$$

In DST, the probability masses are assigned to each subset of Θ. This property allows uncertainty in classification [16].

ICCS Camera Ready Version 2020
To cite this paper please use the final published version:
DOI: 10.1007/978-3-030-50423-6_40

At the first step during the construction of the classifier, each source of evidence i.e. input variable (v) is mapped to a confidence factor $cf(v)$ (0 - 1 scale) using some predefined function derived from the pattern of data distribution. $cf(v)$ is then transformed to BOE as [27]:

$$\begin{aligned} m(\{h\}) &= \frac{B}{(1-A)} cf(v) - \frac{AB}{(1-A)}, \\ m(\{\neg h\}) &= \frac{-B}{(1-A)} cf(v) + B, \\ m(\{h, \neg h\}) &= 1 - m(\{h\}) - m(\{\neg h\}) \end{aligned} \tag{2}$$

In eqn. 2 the value $m(\{h, \neg h\})$ refers the DOB of either belong to a class or not belong to a class. Hence, this value quantify the uncertainty associated with a particular feature (i.e. input variable or evidence). The control variables A and B define the dependence of $m(\{h\})$ on $cf(v)$ and the maximal support for $m(\{h\})$ or $m(\{\neg h\})$. In case of more than one source of evidence for a hypothesis, Dempsters rule of combination is used to combine the individual BOEs to get the final BOE (FBOE) (see [16] for more details). The highest FBOE determine the class label of a sample.

3.4 State-space model construction

Human gait cycle can be broadly classified into four dominant sub-phases: first double limb support (FDLS), single limb support for the left limb (LSL), second double limb support (SDLS), and single limb support for the right limb (RSL) (see fig.2). Based on this, a hypothetical state-space model was proposed (fig. 3) which quantify the temporal evolution of gait signal.

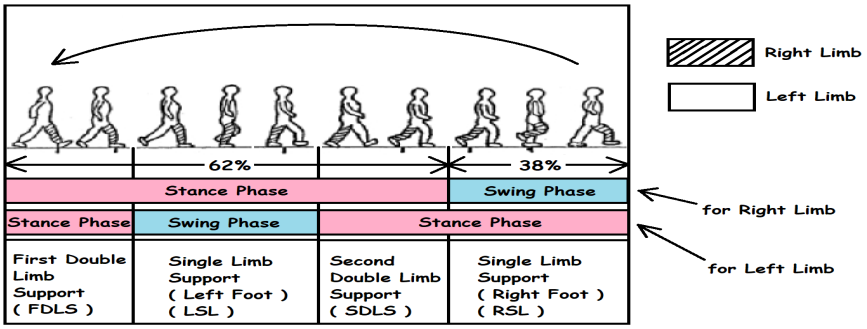

Fig. 2. Sub-phases of a normal gait cycle

For CAwCP, gait velocity was reported as one of the most discrimitive feature [3]. Hence, velocity of both ankle joints (anterior-posterior (A-P) and vertical (V) direction) were selected as the sources of evidence. DST was used as a binary

ICCS Camera Ready Version 2020
To cite this paper please use the final published version:
DOI: 10.1007/978-3-030-50423-6_40

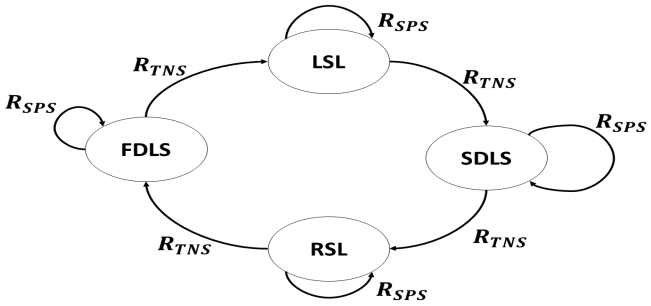

Fig. 3. Hypothetical state-space model

classifier for assigning a frame to a particular state out of two subsequent states. Twenty-one subjects (11 TDCA, 10 CAwCP) were selected for in-sample group (i.e. training set), and remaining (4 TDCA, 5 CAwCP) were selected for out-of-sample (i.e. test set) group. State transition rules was constructed on the basis of elementary hypotheses. The BFOD was defined as: {present state (PS) i.e. hypothesis h, next state (NS) i.e. hypothesis $\neg h$}. Thus the hypothesis space constitutes: $\{\{\varnothing\}, \{PS\}, \{NS\}, \{PS, NS\}\}$. We assumed that the temporal sequence of the states (see fig.3) should not deviate for any subject (both CAwCP and TDCA). Gait cycle was segmented into 4 states (i.e. FDLS,LSL,SDLS,RSL) using the gait event detection algorithm described by Zeni et al. [28]. In order to convert the input variables into confidence factor, we found a suitable probability distribution that fits the best to our input data. Kolmogorov-Smirnov test was performed to investigate the distribution pattern of the input data. Frchet distribution (see eqn.3) was found to fit the best for our input data:

$$cf(v) = e^{-\left(\frac{v-m}{s}\right)^{-\alpha}} \qquad if \quad v > m \tag{3}$$

In eqn.3, $\alpha > 0$ is the shape parameter, m and $s > 0$ are the location and scale parameters respectively. Hence, for each input variable 5 control parameters (i.e. α, m, s, A, B) were considered in this study. For each state, the control parameters, α, m and s, were estimated separately based on the nature of the input variables [10]. Table 2 demonstrates the values assigned to the control variables (i.e. α, m and s) for the FDLS state.

Following the work of Jones et al.[10], the values of A and B were determined using expert knowledge. For individual input variable, the limit of uncertainty was estimated which was used to compute the value of A and B. If for a particular variable v, the upper and lower limit of uncertainty are ϕ_U and ϕ_L respectively, then A and B can be written as [10]:

$$\begin{aligned} A &= \frac{(\phi_U - \phi_L)}{(1 + \phi_U - 2\phi_L)} \\ B &= 1 - \phi_L \end{aligned} \tag{4}$$

ICCS Camera Ready Version 2020
To cite this paper please use the final published version:
DOI: 10.1007/978-3-030-50423-6_40

Table 2. Values of the control variables α, m and s for FDLS state

Input variable	α	m	s
Left ankle (A-P)	5.60	-0.98	1.72
Left ankle (V)	6.04	0.90	1.02
Right ankle (A-P)	7.05	-1.70	2.12
Right ankle (V)	36.91	-8.45	8.72

Inspired by the work of Safranek et al. [27] and jones et al. [10] which considered the input variables as low-level measurements (i.e. assessment which associate substantial level of uncertainty), we assigned 0.98 and 0.2 to ϕ_U and ϕ_L respectively. Hence, in our experiment the value of A and B were 0.49 and 0.80 respectively. Assignment of values to the control variables was performed using in-sample data. BOE of each input variable was then combined to get the FBOE which quantified the support for a frame to assign to a particular state.
It was assumed that a gait cycle can start from any state (out of 4 states). Hence, for the initial time frame of a gait cycle, the FBOE corresponding to all four states were computed. The state having the highest FBOE value was selected as the initial state of the gait cycle. For the subsequent phases the transition of a frame was govern by the following rules:

- R_{SPS}: if FBOE($\{PS\}$) > FBOE($\{NS\}$) + FBOE($\{PS, NS\}$), OR if FBOE ($\{PS\}$) > FBOE($\{NS\}$) but FBOE($\{PS\}$) < FBOE($\{NS\}$) + FBOE ($\{PS, NS\}$), then the corresponding frame will stay at present state;
- R_{TNS}: if FBOE($\{NS\}$) > FBOE($\{PS\}$) but FBOE($\{NS\}$) < FBOE($\{PS\}$) + FBOE($\{PS, NS\}$), then the corresponding frame will transit to the immediate next state.

3.5 Abnormality detection

Dynamic stability, generally quantified by the value of coefficient of variation (CoV) of a feature [29], was reported to be comparatively low for CAwCP population [3]. In order to detect gait abnormality, we computed mean CoV (ω_m) of the time duration for each state for the in-sample group (both CAwCP (ω_m^{ab}) and TDCA (ω_m^n)). The out-sample subjects, used the values of the control variables learned from the in-sample group to compute the corresponding FBOEs. Then the CoV (ω_t) vector for a test subject was estimated. Class label (CL) for an out-sample subject was determined based on $L2$ norm distance as follows:

$$\begin{aligned} \omega_m^n &= \{\omega_{mFDLS}^n, \omega_{mLSL}^n, \omega_{mSDLS}^n, \omega_{mRSL}^n\} \\ \omega_m^{ab} &= \{\omega_{mFDLS}^{ab}, \omega_{mLSL}^{ab}, \omega_{mSDLS}^{ab}, \omega_{mRSL}^{ab}\} \\ \omega_t &= \{\omega_{FDLS}^t, \omega_{LSL}^t, \omega_{SDLS}^t, \omega_{RSL}^t\} \\ CL &= min(L2(\omega_t, \omega_m^{ab}), L2(\omega_t, \omega_m^n)) \end{aligned} \tag{5}$$

Performance of the proposed system was assessed using some classical metrics i.e. accuracy, sensitivity, and specificity. An attempt was also made to quantify the degree of gait abnormality for individual subject using the proposed

ICCS Camera Ready Version 2020
To cite this paper please use the final published version:
DOI: 10.1007/978-3-030-50423-6_40

model. In CP patients, GMFCS level indicates the degree of abnormality [30]. We hypothesized that higher value of CoV of the time duration for each state indicates higher degree of abnormality. Hence, the first abnormality index ($A1$) was computed by taking average of CoV values throughout the 4 states:

$$A1 = \frac{\omega_{FDLS} + \omega_{LSL} + \omega_{SDLS} + \omega_{RSL}}{4} \tag{6}$$

Again, we assumed that more abnormal CP should have higher uncertainty in their gait pattern. On the basis of that we proposed the second abnormality index ($A2$):

$$A2 = \frac{\sum_{i=1}^{N} FBOE(PS, NS)_i}{N} \tag{7}$$

In eqn.7, N refers total number of frames.

4 Results and Discussion

In this study a state-space based automated gait diagnosis system for CAwCP patients was proposed which perform sub-phase wise gait assessment by quantifying feature uncertainty in temporal evolution of gait cycle. Person specific degree of abnormality was also analyzed.

Our proposed model charecterize gait cycle with an average ± 3 frame difference from the corresponding ground truth (for both TDCA and CAwCP). For comparison, we have implemented ML models (i.e. ANN, SVM, and Bayesian classifier) which were used for CP gait abnormality detection in state-of-the-art. The same feature set, used for our state-space construction, was given as input to those models. ANN was implemented with 3-layer architecture (i/p layer nodes:4, o/p layer nodes:1), while for SVM, three kernel functions (i.e. Radial basis function(RBF),polynomial,and linear) were tested. Hyperparameters (ANN: learning rate and hidden nodes; SVM (RBF,polynomial,linear): regularization parameters; SVM (RBF): gamma; SVM (polynomial): degree) was tuned using grid search. In Bayesian classifier, Gaussian mixture model (GMM) was used to approximate the class conditional distribution which was trained using expectation-maximization (EM) algorithm [31]. Leave-one-out cross validation was used to reduce the generalization error. Following the work of Beynon et al. [16] and Jones et al. [10], the belief values obtained from the Cardiff classifier were used for classification also. In that case the FOD was: {normal, abnormal} and FBOE values were used for class labeling.

Our proposed model outperformed state-of-the-art with an overall 87.5% detection accuracy (see table 3). Figure 4 demonstrates the normalized confusion matrix for our proposed model and Cardiff classifier. It can be seen that the false positive value is substantially high for the Cardiff classifier which caused to degrade its performance compared to other classifiers. Deviation of gait pattern of a CAwCP patient from TDCA was not uniform for all phases of a gait cycle. The input feature for the Cardiff classifier characterized an entire gait cycle

ICCS Camera Ready Version 2020
To cite this paper please use the final published version:
DOI: 10.1007/978-3-030-50423-6_40

from where the control parameters were estimated. Hence, the FBOEs, computed using those control parameters, failed to classify correctly some subjects. This might be a cause of lower performance of this classifier. Our state-space model avoids this problem by analyzing the gait sub-phase wise. Specificity is the highest for our model (see table 3), but sensitivity is lower than SVM(RBF) and SVM(linear). This might be due to the varied CP gait pattern, where our model incorrectly performed some state transitions for some of the subjects.

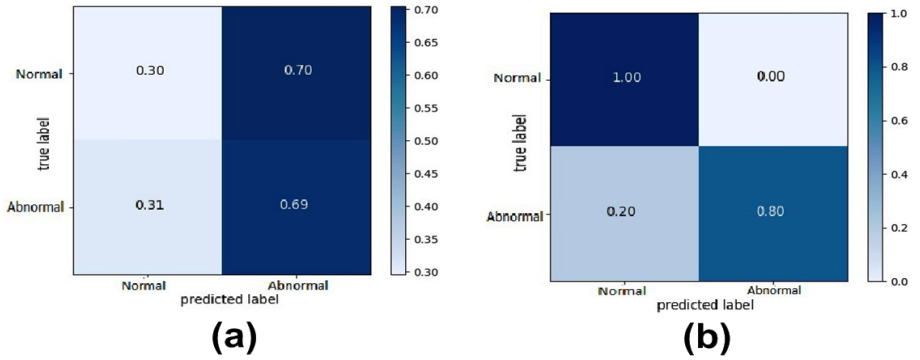

Fig. 4. Normalized confusion matrix. (a) Cardiff classifier, (b) Proposed model

Table 3. Comparative analysis of the proposed model with state-of-the-art

Models	**State-of-the-art**	**Accuracy (%)**	**Sensitivity (%)**	**Specificity (%)**
SVM (RBF)	Kamruzzaman et al. [5]	86.27	92.06	70.67
SVM (Linear)	Zhang et al. [21]	67.12	94.31	40.41
SVM (Polynomial)	Kamruzzaman et al. [5]	61.11	43.26	75.48
ANN	Zhang et al. [21]	67.23	59.43	78.23
Bayesian classifier	Zhang et al.[11]	80.27	72.71	89.32
Cardiff classifier		49.50	49.60	49.20
Proposed		**87.50**	80.00	**100**

In terms of clinical significance, our model also outperformed others by providing a clear interpretation of the results sub-phase wise, whereas, the computation for the other ML models (i.e. ANN,SVM) is basically a 'black-box'. The simplex plots (fig.5(a), 5(b), 5(c), and 5(d)) demonstrate the allocation of data frames in subsequent states during a gait cycle. It can be observed that the transition frame (marked by 'red dot') constitutes high uncertainty which causes it to move to the immediate next state. Uncertainty value then again decreases for which the subsequent frames maps to the next state (which become the current

ICCS Camera Ready Version 2020
To cite this paper please use the final published version:
DOI: 10.1007/978-3-030-50423-6_40

state now). It was noticed that, on an average, the transition frame uncertainty for CAwCP patients is higher than TDCA,

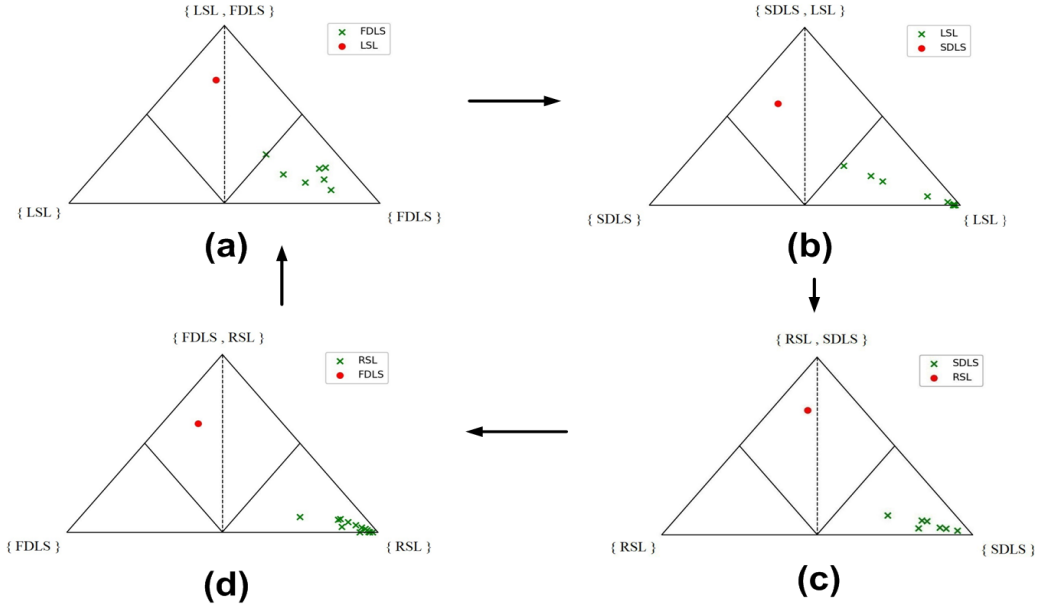

Fig. 5. Simplex plots for a gait cycle of Subj.1 (TDCA). (a) FDLS to LSL, (b) LSL to SDLS, (c) SDLS to RSL, (d) RSL to FDLS

Figure 6 demonstrates sub-phase wise gait distortion of CAwCP compared to TDCA. It shows that CoV of CAwCP differs in FDLS and LSL phases significantly ($\approx 37.5\%$ and $\approx 50\%$) from the corresponding values of TDCA. This information implies that the dynamic stability of CAwCP mainly reduces in this two phases, hence, clinicians should take special attention for these two states during an intervention.

Results in table 4 shows that both $A1$ and $A2$ and consequently the total score are higher for GMFCS II patients than GMFCS I. This implies that dynamic stability decreases in CP patients having higher degree of abnormality. It also demonstrates that CP patients of higher degree associate higher uncertainty value in their gait pattern which may be a consequence to compensate the effect of lower muscle control [3]. The proposed abnormality indexes exhibit promising aspect to quantify the degree of abnormality.

ICCS Camera Ready Version 2020
To cite this paper please use the final published version:
DOI: 10.1007/978-3-030-50423-6_40

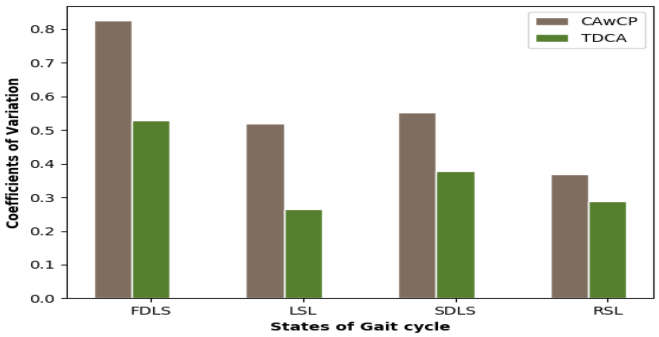

Fig. 6. Sub-phase wise gait assessment

Table 4. Degree of gait abnormality assessment

GMFCS level of CP	Average A1	Average A2	Total score
I	0.5807	0.1394	0.7201
II	0.7997	0.3772	1.1769

5 Conclusion

Automatic gait diagnosis with clinical interpretation is crucial for CAwCP patients. Feature uncertainty takes an important part in abnormal gait detection. The prime contribution of this study is to propose a state-space model which recognize temporal evolution of gait pattern by quantifying feature uncertainty. Data were captured using a low-cost multi-Kinect setup which provided the standard 10 meter walking path. An attempt was also made to quantify the degree of abnormality by proposing abnormality indexes. Results shows that the performance of our model is comparable with state-of-the-art. As a future research aspect, some data-driven constraints may be imposed on the state transition rules to further reduce the frame offset (frame difference from the ground truth) of our model. Investigating the performance of the proposed system in detecting CAwCP gait in more challenged environment (i.e. duel task walking, walking on uneven ground) seems warrented. The proposed model performs sub-phase wise gait assessment and provides succinct interpretability of the results which will help the clinicians in decision making during rehabilitation treatment.

Acknowledgment

We would like to be extremely thankful to Science and Engineering Research Board (SERB), DST, Govt. of India (FILE NO: ECR/2017/000408) to partially support this research work. We also like to thank IICP, Kolkata for providing Cerebral Palsy patients and necessary arrangements to collect data.

ICCS Camera Ready Version 2020
To cite this paper please use the final published version:
DOI: 10.1007/978-3-030-50423-6_40

References

1. Carol L Richards and Francine Malouin. Cerebral palsy: definition, assessment and rehabilitation. In *Handbook of clinical neurology*, volume 111, pages 183–195. Elsevier, 2013.
2. Moshe Stavsky, Omer Mor, Salvatore Andrea Mastrolia, Shirley Greenbaum, Nandor Gabor Than, and Offer Erez. Cerebral palsytrends in epidemiology and recent development in prenatal mechanisms of disease, treatment, and prevention. *Frontiers in pediatrics*, 5:21, 2017.
3. Saikat Chakraborty, Anup Nandy, and Trisha M Kesar. Gait deficits and dynamic stability in children and adolescents with cerebral palsy: A systematic review and meta-analysis. *Clinical Biomechanics*, 71:11–23, 2020.
4. Nicola Smania, Paola Bonetti, Marialuisa Gandolfi, Alessandro Cosentino, Andreas Waldner, Stefan Hesse, Cordula Werner, Giulia Bisoffi, Christian Geroin, and Daniele Munari. Improved gait after repetitive locomotor training in children with cerebral palsy. *American journal of physical medicine & rehabilitation*, 90(2):137–149, 2011.
5. Joarder Kamruzzaman and Rezaul K Begg. Support vector machines and other pattern recognition approaches to the diagnosis of cerebral palsy gait. *IEEE Transactions on Biomedical Engineering*, 53(12):2479–2490, 2006.
6. Leilani H Gilpin, David Bau, Ben Z Yuan, Ayesha Bajwa, Michael Specter, and Lalana Kagal. Explaining explanations: An overview of interpretability of machine learning. In *2018 IEEE 5th International Conference on data science and advanced analytics (DSAA)*, pages 80–89. IEEE, 2018.
7. Leo Breiman. Statistical modeling: The two cultures (with comments and a rejoinder by the author). *Statistical science*, 16(3):199–231, 2001.
8. H Ma and WH Liao. Human gait modeling and analysis using a semi-markov process with ground reaction forces. *IEEE transactions on neural systems and rehabilitation engineering: a publication of the IEEE Engineering in Medicine and Biology Society*, 25(6):597–607, 2017.
9. Richard EA van Emmerik, Scott W Ducharme, Avelino C Amado, and Joseph Hamill. Comparing dynamical systems concepts and techniques for biomechanical analysis. *Journal of Sport and Health Science*, 5(1):3–13, 2016.
10. Lianne Jones, Malcolm J Beynon, Catherine A Holt, and Stuart Roy. An application of the dempster–shafer theory of evidence to the classification of knee function and detection of improvement due to total knee replacement surgery. *Journal of biomechanics*, 39(13):2512–2520, 2006.
11. Bai-ling Zhang, Yanchun Zhang, and Rezaul K Begg. Gait classification in children with cerebral palsy by bayesian approach. *Pattern Recognition*, 42(4):581–586, 2009.
12. Tinne De Laet, Eirini Papageorgiou, Angela Nieuwenhuys, and Kaat Desloovere. Does expert knowledge improve automatic probabilistic classification of gait joint motion patterns in children with cerebral palsy? *PloS one*, 12(6), 2017.
13. Sebastian Wolf, Tobias Loose, Matthias Schablowski, Leonhard Döderlein, Rüdiger Rupp, Hans Jürgen Gerner, Georg Bretthauer, and Ralf Mikut. Automated feature assessment in instrumented gait analysis. *Gait & Posture*, 23(3):331–338, 2006.
14. Arthur P Dempster. A generalization of bayesian inference. *Journal of the Royal Statistical Society: Series B (Methodological)*, 30(2):205–232, 1968.
15. Glenn Shafer. *A mathematical theory of evidence*, volume 42. Princeton university press, 1976.

ICCS Camera Ready Version 2020
To cite this paper please use the final published version:
DOI: 10.1007/978-3-030-50423-6_40

16. Malcolm J Beynon, Lianne Jones, and Catherine A Holt. Classification of osteoarthritic and normal knee function using three-dimensional motion analysis and the dempster-shafer theory of evidence. *IEEE Transactions on Systems, Man, and Cybernetics-Part A: Systems and Humans*, 36(1):173–186, 2005.
17. PR Biggs, GM Whatling, C Wilson, and CA Holt. Correlations between patient-perceived outcome and objectively-measured biomechanical change following total knee replacement. *Gait & posture*, 70:65–70, 2019.
18. Ming Liu, Fan Zhang, Philip Datseris, and He Helen Huang. Improving finite state impedance control of active-transfemoral prosthesis using dempster-shafer based state transition rules. *Journal of Intelligent & Robotic Systems*, 76(3-4):461–474, 2014.
19. Leen Van Gestel, Tinne De Laet, Enrico Di Lello, Herman Bruyninckx, Guy Molenaers, Anja Van Campenhout, Erwin Aertbeliën, Mike Schwartz, Hans Wambacq, Paul De Cock, et al. Probabilistic gait classification in children with cerebral palsy: A bayesian approach. *Research in developmental disabilities*, 32(6):2542–2552, 2011.
20. Angela Nieuwenhuys, Sylvia Õunpuu, Anja Van Campenhout, Tim Theologis, Josse De Cat, Jean Stout, Guy Molenaers, Tinne De Laet, and Kaat Desloovere. Identification of joint patterns during gait in children with cerebral palsy: a delphi consensus study. *Developmental Medicine & Child Neurology*, 58(3):306–313, 2016.
21. Yanxin Zhang and Ye Ma. Application of supervised machine learning algorithms in the classification of sagittal gait patterns of cerebral palsy children with spastic diplegia. *Computers in biology and medicine*, 106:33–39, 2019.
22. Joseph J Krzak, Daniel M Corcos, Diane L Damiano, Adam Graf, Donald Hedeker, Peter A Smith, and Gerald F Harris. Kinematic foot types in youth with equinovarus secondary to hemiplegia. *Gait & posture*, 41(2):402–408, 2015.
23. Fiona Dobson, Meg E Morris, Richard Baker, and H Kerr Graham. Gait classification in children with cerebral palsy: a systematic review. *Gait & posture*, 25(1):140–152, 2007.
24. Eirini Papageorgiou, Angela Nieuwenhuys, Ines Vandekerckhove, Anja Van Campenhout, Els Ortibus, and Kaat Desloovere. Systematic review on gait classifications in children with cerebral palsy: an update. *Gait & posture*, 69:209–223, 2019.
25. Daphne J Geerse, Bert H Coolen, and Melvyn Roerdink. Kinematic validation of a multi-kinect v2 instrumented 10-meter walkway for quantitative gait assessments. *PloS one*, 10(10):e0139913, 2015.
26. Björn Müller, Winfried Ilg, Martin A Giese, and Nicolas Ludolph. Validation of enhanced kinect sensor based motion capturing for gait assessment. *PloS one*, 12(4):e0175813, 2017.
27. Robert J Safranek, Susan Gottschlich, and Avinash C Kak. Evidence accumulation using binary frames of discernment for verification vision. *IEEE Transactions on Robotics and Automation*, 6(4):405–417, 1990.
28. JA Zeni Jr, JG Richards, and JS Higginson. Two simple methods for determining gait events during treadmill and overground walking using kinematic data. *Gait & posture*, 27(4):710–714, 2008.
29. Jeffrey M Hausdorff. Gait dynamics, fractals and falls: finding meaning in the stride-to-stride fluctuations of human walking. *Human movement science*, 26(4):555–589, 2007.
30. Susan A Rethlefsen, Deirdre D Ryan, and Robert M Kay. Classification systems in cerebral palsy. *Orthopedic Clinics*, 41(4):457–467, 2010.
31. Richard O Duda, Peter E Hart, and David G Stork. *Pattern classification*. John Wiley & Sons, 2012.

ICCS Camera Ready Version 2020
To cite this paper please use the final published version:
DOI: 10.1007/978-3-030-50423-6_40